THE JOURNAL OF PHYSICAL CHEMISTRY B

 VOLUME 113, NUMBER 49, DECEMBER 10, 2009

ARTICLES

Slow Solvation Dynamics in the Microheterogeneous Water Channels of Nafion Membranes

Tarak Nath Burai and Anindya Datta*

Department of Chemistry, Indian Institute of Technology Bombay, Powai, Mumbai 400 076, India

Received: August 15, 2009; Revised Manuscript Received: September 21, 2009

Solvation dynamics in Nafion membrane is studied using the well-known solvation probe, coumarin 102 (C102). In native Nafion membrane, the fluorescence maximum of C102 occurs at 525 nm. The decays recorded at different wavelengths are superimposable. There is no time-dependent Stokes shift (TDSS) in the time scale of the experiment. This is rationalized in light of the strongly acidic environment in Nafion membrane, which causes the C102 molecules to become protonated. The protonated molecules are bound tightly to the negatively charged sulfonate groups. In Na^+- and Me_4N^+-exchanged Nafion membranes, the fluorescence gets blue-shifted by 65 nm, indicating the deprotonation of the cation and formation of neutral C102 in these membranes. TDSS is observed in the picosecond−nanosecond time scale, in the cation-exchanged Nafion membranes, although the amount of Stokes' shift is rather small, as compared to that observed in organic solvents, indicating that a significant amount of the solvation is ultrafast and is missed in the present experiment. The observed solvation dynamics is bimodal with fast (∼1 ns) and slow (>10 ns) components. The ultraslow component is ascribed to the quasi-static water molecules in the Nafion membrane. The difference in the extents of apparently missing ultrafast components, between Me_4N^+- and Na^+-substituted membranes is rationalized by a model involving the difference in distributions of the cations in the water channel.

Introduction

Nafion is a well-known proton transfer membrane.[1] It consists of pendant sulfonate groups attached to a fluorocarbon backbone, rendering it a reverse micelle-like structure. Molecular dynamics simulations have identified two kinds of dynamics of water and hydronium ions: fast and slow, in subpicosecond and picosecond time domains, respectively.[2] This observation is explained in terms of the presence of bound and free water molecules, using an extension of the proton hopping model proposed by Laage and Hynes[3] and considering the hydrogen bond dynamics involved.[4] NMR studies reveal the presence of free and bound water molecules in Nafion.[5] FT-IR study reveals the water molecules close to the interfacial region exhibit an O−H stretching vibration at 3668 cm^{-1}, whereas the O−H stretching occurs at 3500 cm^{-1} for the free molecules.[6] Recently, it has been reported that the interfacial structure of Nafion is dependent on the level of hydration, unlike the well-known aerosol OT reverse micelles, with which it is often compared due to the apparent similarity in the microscopic structures.[4]

The water inside the Nafion membrane is highly acidic in nature.[7−9] It is possible to regulate the water content as well as the acidity quite easily by the incorporation of organic and inorganic cations.[5,10−13] This is manifested in an early study from our group, in which the extent of excited state proton transfer (ESPT) in 2-(2′-pyridyl)benzimidazole (2PBI) is regulated by cation exchange.[14] The ESPT in 2PBI is known to occur in acidic solutions.[15] In Nafion, it was observed that the ESPT is

* To whom correspondence should be addressed. Phone: +91 22 2576 7149. Fax: + 91 22 2572 3480. E-mail: anindya@chem.iitb.ac.in.

10.1021/jp907902t CCC: $40.75
Published on Web 11/11/2009

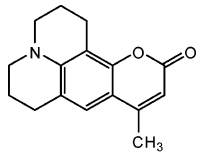

C-102

Figure 1. Chemical structures of Coumarin 102 (C102)

extensive due to the superacidity of the membrane. Upon cation exchange, the ESPT was hindered due to the lower acidity of the membrane. Moreover, at same concentrations, bulky tetramethyl ammonium cations were found to hinder ESPT to a greater extent than the smaller sodium ions. This was explained by the displacement of a greater amount of water by the bulkier cation. The bound water molecules are not expected to be displaced easily by simple cation exchange, so it is likely that the displaced water molecules are essentially from the pool of "free" water molecules. Moreover, the hydration numbers of the cations that replace H_3O^+ are different from that of H_3O^+ itself. Distribution of cations is another important factor that needs to be reckoned in this context. An interplay of these factors is expected to lead to an alteration of slow solvation dynamics that is often observed in microheterogeneous media,[16] as a result of a dynamic equilibrium between bound and free water molecules in such media.[17] The dynamics of the water in the water channel of Nafion is remarkably similar to that of the water in the water pool of aerosol OT microemulsions, as has been reported in a study of deprotonation dynamics of a photoacid in the water channels of Nafion.[18]

This is the motivation for the work reported here. Solvation dynamics has been studied in Nafion membranes by monitoring the time-dependent Stokes' shift (TDSS) of Coumarin 120 (C120, Figure 1), which is used widely for this purpose.[19−24] Since Nafion is a superacid, it is likely to protonate C102, which is reported to exist as a cation in very acidic media.[25] At comparatively higher pH, such as pH = 2, it is neutral in the ground electronic state, but gets protonated in the electronically excited state.[26,27] The well-studied acid−base properties, in ground and excited states, are considered in the discussion of the interplay of the modulation of acidity and water content in the Nafion membranes by cation exchange.

Experimental Section

Coumarin 102 (Radiant Dyes, USA, laser grade) was used as received. Nafion-117 membrane of a thickness of 0.007 in., from Sigma-Aldrich, was carefully cleaned by placing in concentrated HNO_3 and stirring at 60 °C for 24 h. The film was then washed thoroughly with double-distilled water. The Na^+- and Me_4N^+-exchanged membranes were prepared by stirring the acid-washed membrane in a concentrated NaOH solution or Me_4NCl (TMAC) solution, respectively, for 24 h to reach complete equilibrium. The excess base on the surface of the Na^+-exchanged membrane was removed by repeated washing with doubly distilled water. The C102 was incorporated into the swollen Nafion membrane by keeping the membrane for 24 h in C102 solution. After loading, and prior to measurements, the membranes were rinsed with doubly distilled water. The amount of C102 loaded into the membrane was kept sufficiently low by ensuring that the optical density of the doped membrane was lower than 0.2 at λ_{max}^{abs}.

The steady state spectra were recorded on JASCO V530 spectrophotometer and Varian Cary Eclipse fluorometer. Time-resolved fluorescence measurements were performed using a picosecond pulsed diode laser and light-emitting-diode-based TCSPC fluorescence spectrometer with $\lambda_{ex} = 406$ and 341 nm, respectively, using a MCP-PMT as the detector. The emission from the samples was collected at a right angle to the direction of the excitation beam, at magic angle polarization (54.7°), except for the anisotropy measurements. The full width at half-maximum of the instrument response function was 250 ps for 406 nm and 800 ps for 341 nm. The data were fitted to multiexponential functions after deconvolution of the instrument response function by an iterative reconvolution technique, using the IBH DAS 6.2 data analysis software, in which reduced χ^2 and weighted residuals serve as parameters for goodness of fit.[28]

Time resolved emission spectra (TRES) and the solvation correlation function, $C(t)$ have been constructed from the steady state and time-resolved fluorescence data. To construct the TRES, the fluorescence decays have been recorded across the emission spectrum (430−530 nm) at intervals of 8 nm with a bandpass of 2 nm. The fitted fluorescence decays have been scaled with the steady state fluorescence intensities following the usual procedure.[29−31] The fractional contribution of each component to the fluorescence spectrum at the wavelength of measurement ($I_i(\lambda) = a_i\tau_i/\sum_i a_i\tau_i$, where $I_i(\lambda)$ is the fractional contribution, and a_i and τ_i are the relative amplitude and lifetime of the ith component, respectively) was calculated. Reconstruction of the time-resolved spectra was performed following the procedure described by Maroncelli and Fleming.[32] Then using the parameters of the best fit to the fluorescence decays, time-resolved spectra at different times, t, were generated by fitting the data to a log-normal function to get the peak frequency $\upsilon(t)$. Hence, the solvent correlation function, $C(t)$ was constructed. $C(t)$ is defined as[32]

$$C(t) = \frac{\upsilon(t) - \upsilon(\infty)}{\upsilon(0) - \upsilon(\infty)} \tag{1}$$

where $\upsilon(0)$, $\upsilon(t)$, and $\upsilon(\infty)$ are, respectively, the emission frequencies at time 0, t, and ∞. [$\upsilon(\infty)$ represents the spectrum of the probe molecule after solvation is complete.[33,34]] Generally, $C(t)$ decays with time, following a multiexponential decay law:

$$C(t) = \sum_i a_i e^{-t/\tau_i} \tag{2}$$

where τ_i denotes a solvation time. If the solvation is so slow that it does not get completed within the lifetime of the fluorophore, then determination of $\upsilon(\infty)$ becomes difficult. There are several views on the appropriate choice of $\upsilon(\infty)$. In the present work, $\upsilon(\infty)$ is taken to be the steady state fluorescence maximum.[40]

The time-dependent anisotropy, $r(t)$, is constructed from the decays at directions parallel and perpendicular to that of the excitation polarization ($I_{II}(t)$ and $I_I(t)$ respectively).[35] The decays of $r(t)$ are fitted to single and multiexponential functions, as required, using the formula

$$r(t) = r_0 \sum_i a_i \exp\left(-\frac{t}{(\tau_r)_i}\right) \tag{3}$$

where r_0 is the fundamental anisotropy in the absence of other depolarizing processes, such as rotational diffusion or energy transfer.

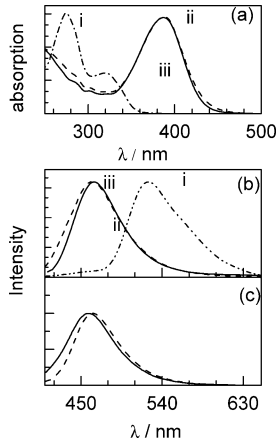

Figure 2. Peak normalized (a) Absorption spectra and (b) emission spectra of C102 in (i) native (— • —), (ii) Me_4N^+-loaded (— — —), and (iii) Na^+-loaded Nafion (—) with $\lambda_{ex} = 350$ and 380 nm for native and cation-exchanged membranes, respectively. (c) Emission spectra of C102 in Me_4N^+-loaded Nafion at $\lambda_{ex} = 341$ nm (—) and 406 nm (— — —).

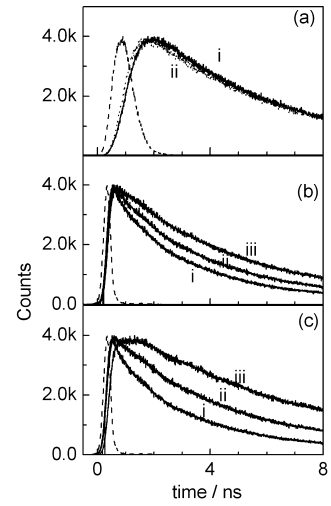

Figure 3. Fluorescence decays of (a) native Nafion at different emission wavelengths (i) 500 and (ii) 600. $\lambda_{ex} = 341$ nm. (b) Me_4N^+-loaded Nafion membrane (c) Na^+-loaded Nafion at different emission wavelengths (i) 430, (ii) 460, and (iii) 550 nm. $\lambda_{ex} = 406$ nm.

Results and Discussion

1. Steady-State Spectra. The steady-state absorption and emission spectra of C102 in HNO_3-washed Nafion film and Na^+ and Me_4N^+-exchanged Nafion membrane are shown in Figure 2. In all the cases, the excitation spectra are superimposable with the absorption spectra. The steady state absorption spectrum of C102 in HNO_3-washed Nafion membrane consists of a higher frequency absorption band (275 nm) and a minor band at 320 nm. This is similar to the absorption spectrum of C102 in ethanol, in the presence of 3.33 mol/L H_2SO_4, where the ground state species is the cation $C102H^+$, the nitrogen atom of which is protonated. Earlier computational studies on C102 in ethanol had identified the lowest-lying state to be a $\pi-\pi^*$ state (energy difference being equivalent to a wavelength of 275 nm) with small oscillator strength. This state has contributions from nearly degenerate HOMO-1 → LUMO and HOMO → LUMO + 1 transitions.[36] This theoretically assigned 275 nm band is located in the experimental spectrum at 275 nm with high intensity, in the native Nafion film. Thus, C102 is found to be protonated in native Nafion, which is highly acidic. This is analogous to our earlier observation with 2-(2′-pyridyl)benzimidazole (2PBI) in Nafion.[14,15] On performing cation exchange by NaOH and Me_4NCl, the absorption spectra resemble that in an aqueous solution, in which the absorption maximum occurs at 390 nm.[37]

The emission maximum in native Nafion occurs at 525 nm, indicating that the emitting species is the cation, in which the positive charge is on the oxygen atom. This species is believed to form from the N-protonated cation as a result of excited state proton transfer.[17] In the Na^+- and Me_4N^+-exchanged Nafion membrane, the emission maximum shifts to 460 nm (Figure 2b). It can be mentioned here that in neutral, aqueous solutions of C102, the emission maximum occurs at 490 nm, the emission quantum yield (ϕ_f) being 0.12,[37] so the predominant emissive species in the cation-exchanged films is found to be neutral C102. The blue shift of 30 nm in emission, as compared to that in neutral, aqueous solution, may be rationalized in terms of the lower polarity of the water in the water pools of Nafion. The emission maximum of C102 in ethanol is 467 nm, which is fairly close to that observed in the present experiment. Therefore, it can be inferred that in the membrane, C102 experiences a micropolarity that is smiliar to the polarity of ethanol. Notably, the emission spectrum in the Me_4N^+-substituted membrane depends on the excitation wavelength (Figure 2c), whereas no such excitation wavelength dependence is observed in Na^+-substituted membrane (data not shown). The reason for this excitation wavelength dependence is discussed later in this article.

TABLE 1: Time-Resolved Parameter of C102 in Native and Cation-Exchanged Membranes

λ_{ex} (nm)	Nafion membrane	λ_{em} (nm)	τ_1 (ns)	τ_2 (ns)	a_1	a_2
	native	500		5.00		
		525		5.00		
		600		5.00		
	Me_4N^+-exchanged	420	0.63	4.11	0.18	0.82
341		460	2.60	5.05	0.03	0.97
		530	0.62	5.58	−0.42	1.42
	Na^+-exchanged	420	1.23	4.26	0.35	0.65
		460	0.55	5.60	0.10	0.90
		530	0.90	6.70	−0.35	1.35
	Me_4N^+-exchanged	430	1.23	3.80	0.38	0.62
		460	1.26	5.10	0.07	0.93
		530	0.50	5.66	−0.17	1.17
406	Na^+-exchanged	430	1.21	4.01	0.40	0.60
		460	1.63	5.27	0.26	0.74
		530	0.48	6.44	−0.14	1.14

2. Slow Solvation Dynamics in Cation-Exchanged Membranes. The fluorescence decays of C102 in the native Nafion membrane are emission-wavelength-independent (Figure 3a, Table 1). The lifetime of C102 in native Nafion membrane is 5 ns. This is greater than the lifetime of 3 ns observed in aqueous solution (pH = 1). The longer lifetime of the excited state might have arisen out of the electrostatic interaction of the cationic excited state with the negative sulfonate groups of Nafion. However, the decays in Na^+- and Me_4N^+-exchanged Nafion film are found to be very strongly dependent on the emission wavelengths with excitation at $\lambda_{ex} = 406$ nm (Table 1). The trace at the red end is associated with a rise, whereas at the blue end, a fast decay is observed (Figure 3b, c). The trace in Na^+-exchanged Nafion membrane at the red end (530 nm) is fitted to a biexponential function, with a rise time of 0.5 ns and a decay of 6.5 ns, whereas at the blue end (430 nm), biexponential decay with an average lifetime of 3.0 ns is observed. Such fast decay at the blue end and rise at the red end is typical of fluorescent probes undergoing solvation within

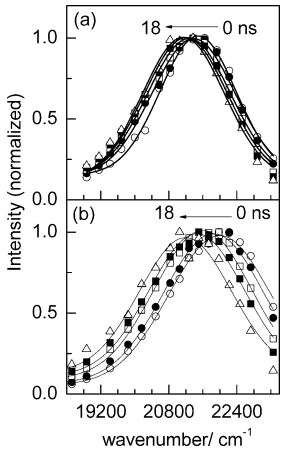

Figure 4. Time-resolved emission spectra of C102 in (a) Me_4N^+-exchanged Nafion film. (b) Na^+-exchanged Nafion film at 0 (○), 1 (560), 5 (□), and 10 (■), and 18 ns (△).

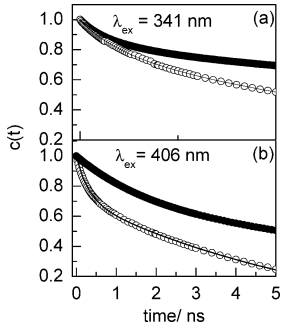

Figure 5. Decay of response function, $C(t)$ of C102 in Na^+- (●) and Me_4N^+-exchanged (○) Nafion membrane for (a) $\lambda_{ex} = 341$ nm and (b) $\lambda_{ex} = 406$ nm. The points denote the actual values of $C(t)$, and the solid line denotes the best fit to a biexponential decay.

TABLE 2: The Decay Parameters of $C(t)$ in Cation Exchanged Nafion Membrane

Nafion membrane	λ_{ex} (nm)	$\upsilon(0)$ cm^{-1}	$\Delta\upsilon^{obs}$ [a] (cm^{-1})	τ_1 [b] (ns)	a_1 (%)	τ_2 [b] (ns)	a_2 (%)
Me_4N^+-exchanged membrane	341	21 660	425	1.00	18	12	82
	406	21 495	350	0.32	24	7	76
Na^+-exchanged membrane	341	22 034	785	0.76	28	16	72
	406	22 002	810	1.70	22	20	78

[a] ±100 cm^{-1}. [b] ±10%.

the time scale of measurement.[32] Thus, C102 is found to experience a markedly different microenvironment in the cation-exchanged membranes than in the native membrane. The time-resolved emission spectra are constructed as described in the experimental section from the fluorescence decays and the steady state emission spectra (Figure 4).

The decays of $C(t)$ are shown in Figure 5, and the decay parameters are summarized in Table 2. $C(t)$ is fitted to a biexponential function to obtain the solvations times (Table 2). The slow process constitutes ~24 and 22% of the total solvation response in Me_4N^+- and Na^+-exchanged Nafion membrane at λ_{ex} 406 nm. This leads to an average solvation time $\langle\tau_s\rangle = a_1\tau_1 + a_2\tau_2 = 5.4$ and 15.94 ns at λ_{ex} 406 nm and 10 and 11.73 ns at λ_{ex} 341 nm, in Me_4N^+- and Na^+-exchanged Nafion film, respectively. The dynamic Stokes shift of C102 observed in the case of the Me_4N^+-exchanged Nafion membrane (425 cm^{-1} at $\lambda_{ex} = 341$ nm, 350 cm^{-1} at λ_{ex} 406 nm) is much smaller than that obtained in Na^+-exchanged Nafion membrane. Both values are considerably smaller than the Stokes shift observed for C102 in neat water[38,39] or even in other microheterogeneous media.[19,20] The component of solvation that has been missed in the experiment may have arisen for the following reasons: the missed ultrafast component of solvation dynamics[33] and an ultraslow component of solvation that is not complete within the excited state lifetime of the fluorophore, leading to an uncertainty in $\nu(\infty)$.

The $\nu(0)$ values obtained here (Table 2) are considerably lower in energy as compared to the estimated zero-time emission maxima of this fluorophore in microheterogeneous media.[40] Therefore, a major portion of the solvation is found to occur in an ultrafast time scale that is not detectable in the TCSPC experiment. This ultrafast solvation is likely to be ascribed to the "bulklike" water molecules that reside in the water channels at a distance from the pendant SO_3^- groups. Notably, the size of the water channels is comparable to that of the large water pools of microemulsions that have high water contents, so a bulklike behavior may be expected. Interestingly, the amount of missed component, as estimated from the $\nu(0)$ value (Table 2) is greater in the Me_4N^+-substituted membrane, indicating that the Coumarin 102 molecules sense a greater amount of bulklike water in it, as compared to that in the Na^+-exchanged membrane. This is seemingly contrary to the expectation that Me_4N^+ ions would displace a greater amount of water than an equal amount of smaller Na^+ ions. A possible explanation of this phenomenon is that the Na^+ ions are distributed more uniformly within the water channel as compared to the bulky and less hydrophilic Me_4N^+ ions, which are likely to reside primarily near the periphery of the water channels at a distance from the center of the water channels (Scheme 1), thereby forming a tighter electrical double layer. The positive charge on the Me_4N^+ ions enables them to reside near the negatively charged interface, due to electrostatic attraction. The interplay of electrostatic and hydrophobic effects is known to be important in determining the interspecies interactions in situations like these.[41]

Therefore, the C102 molecules are located in the water channel, away from the SO_3^- groups, to a greater extent in the Me_4N^+-substituted membrane than in the Na^+-substituted membranes. Consequently, the fluorescent probe experiences a greater fraction of "bulk-water-like" ultrafast dynamics. Excitaion at 341 nm yields a slightly smaller amount of contribution from the missing ultrafast component for C102 in the Me_4N^+-substituted membrane, as compared to excitation at 406 nm (Table 2). This observation is in line with the proposed explanation, because 406 nm is absorbed predominantly by C102 molecules that reside in a waterlike environment, and 341 nm is absorbed to a greater extent by the molecules in the interfacial region. The seemingly greater contribution of the ultrafast dynamics in Me_4N^+-substituted membrane upon excitation at 406 nm indicates that the inhomogeneity in the environment is more prominent in this membrane as compared to the Na^+-substituted membrane and explains the excitation wavelength dependence of the emission spectra in the Me_4N^+-substituted membrane (Figure 2c).

The observed slow solvation dynamics can be explained by the well-established model involving bound and free water molecules. The decay of $C(t)$ is bimodal (Table 2, Figure 5), similar to earlier reports in microheterogeneous media.[42,43] The absence of the slow dynamics in the native membrane is rationalized as follows: The cationic form of C102, formed predominantly in the native membrane, appears to be closely associated with the sulfonate groups and does not exhibit the time-dependent Stokes shift, because the water cluster in the hanging side chain is held immobile by a hydrogen bond network in the presence of cationic species sticking to the

SCHEME 1: Distribution of C102 (ovals) in (A) Me_4N^+- (light circles) and (B) Na^+-Substituted (ringed circles) Nafion Membrane

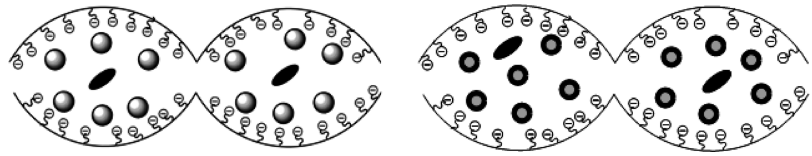

sulfonate group. This is analogous to the static hydration layer that plays a significant role in the stability and function of the proteins by covering the surface of the proteins.[44] Hence, slow solvation dynamics is not observed in the native Nafion membrane.

Upon cation exchange, the acidity of the membrane decreases, and the neutral C102 molecules predominate, as is manifested in the absorption and fluorescence spectra. These neutral species are no longer tightly associated with the pendant sulfonate groups and, hence, can report the slow dynamics, similar to the situation in other microheterogeneous media. The excitation wavelength dependence of the solvation dynamics (Figure 5, Table 2) is reminiscent of that observed by Bhattacharyya and co-workers in the triblock copolymer $(PEO)_{20}-(PPO)_{20}-(PEO)_{20}$ in the absence and the presence of sodium dodecyle sulfate due to the polarity distribution between the core and corona region.[45] In the present context, excitation at 341 nm yields a slower dynamics because this wavelength is absorbed predominantly by C102 molecules nearer to the interface, whereas 406 nm is likely to be absorbed by C102 in the aqueous core, as discussed earlier in this manuscript. Interestingly, a very long component of 7−16 ns is observed in both cation-exchanged membranes. This ultraslow solvation dynamics is consistent with the dielectric relaxation studies on biological water, whose dielectric relaxation is bimodal, with one component of 10 ps that is the longitudinal dielectric relaxation time (τ_L) of ordinary water and another of about 10 ns.[46]

Using dielectric relaxation spectroscopy, Maniasa and co-workers recently reported the nature of three types of water in acid-form Nafion 117.[47] For the first type of water molecules, a picosecond relaxation observed is identified with the cooperative motion of free water. The second type of water molecules strongly bound to the charged sulfonic groups shows the slowest process (microsecond relaxation times), and a third type of water molecules identified as loosely bound water containing substantial dynamical heterogeneities is characterized by picosecond relaxation times, close to and about three times slower than those of bulk water. We ascribe the slowest component of solvation to the quasi-static water molecules, and the slow (hundreds of picoseconds) component can be rationalized by using the Bagchi model.[17]

3. Fluorescence Anisotropy Decays. The anisotropy decay in native Nafion is fitted well monoexponentially with eq 1 (Figure 6). The fitted value of decay of C102 in native Nafion membrane is 3 ns. However, decays in cation-exchanged Nafion membrane is fitted with a hindered rotor model according to the following equation as

$$r(t) = \{r(0) - r(\alpha)\}[a_{fast}\exp(-t/\tau_{fast}) + a_{slow}\exp(-t/\tau_{slow})] + r(\alpha) \quad (4)$$

The fitted value of decays of C102 in Me_4N^+-exchanged Nafion membrane at λ_{ex}= 406 nm, are τ_{fast} = 0.18 ns (70%) and τ_{slow} = 7 ns (30%). The residual anisotropy (r_∞) is 0.25. The high residual anisotropy indicates the hindered rotation of the C102 molecules.[48] The decays of C102 in Na^+-exchanged Nafion membrane are almost superimposable with those in the Me_4N^+-exchanged membranes. Notably, the $r(0)$ value in the native membrane is markedly less than 0.4, whereas it is 0.4 in the cation-exchanged membranes (Figure 6). The lower $r(0)$ value in the native membranes is in line with the excited state proton transfer that is reported for C102 in highly acidic media. The residual anisotropy indicates that a signifant number of C102 molecules experience an environment whose relaxation is not complete within the lifetime of the fluorophore. This is in agreement with the ultraslow solvation dynamics observed in the cation-substituted membranes. The anisotropy decays in Me_4N^+-exchanged Nafion membrane have been recorded using both excitation wavelengths (Figure 6). The short component of depolarization, upon 341 nm excitation, is 0.40 ns, as compared with a value of 0.18 ns at 406 nm excitation. Thus, the depolarization is slower upon excitation at 341 nm, and this bolsters the contention that 341 nm light is absorbed primarily by fluorophores near the periphery and 406 nm light is absorbed primarily by fluorophores residing near the center of the water channels.

Conclusion

TDSS of Coumarin 102 is not observed in native Nafion because cationic C102 molecules are tightly bound to the sulfonate group pendent with the fluorocarbon backbone. However, TDSS is observed upon regulation of the acidity of the membrane by exchanging the H_3O^+ ions with Na^+ and Me_4N^+ cations. The observed solvation dynamics in the cation-exchanged membranes are bimodal, with two components of 0.32 and 7 ns for Me_4N^+-exchanged film and 1.7 ns, 20 ns for Na^+ exchanged film at λ_{ex}= 406 nm. The lower value of $r(0)$ for C102 in native membrane is in line with the excited state proton transfer that is reported for C102 in highly acidic media. The residual anisotropy indicates that relaxation of the environment around the C102 is not complete within the excited state lifetime of the fluorophore. Thus, the water channels of Nafion are found to consist of at least two different regions: the water molecules near the sulfonate groups exhibit the typical slow and ultraslow dynamics observed in microheterogeneous media, whereas the aqueous core appears to exhibit bulk-water-like

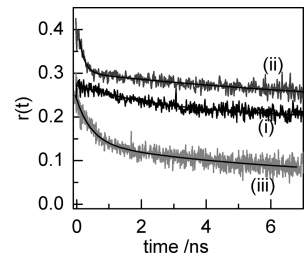

Figure 6. Fluorescence anisotropy decay of C102 at (i) native Nafion, λ_{em} = 525 nm, λ_{ex} = 341 nm and (ii, iii) Me_4N^+-exchanged Nafion λ_{em} = 460 nm, and λ_{ex} = 406 and 341 nm, respectively. The solid lines denote the best fit to the experimental data.

ultrafast relaxation. This is in line with the difference between the interfacial region and the core region of the water channels, observed earlier by Fayer and co-workers.[4,18] Na^+- and Me_4N^+-substituted membranes appear to have very different distributions of the cations in the water channel because the apparent $\nu(0)$ values are different in the two membranes.

Acknowledgment. This work is supported by the SERC DST Grant no. SR/S-1/PC-19/2005 to A.D. T.N.B. thanks CSIR for a SRFship. The authors thank the reviewer for insightful comments.

References and Notes

(1) Mauritz, K. A.; Moore, R. B. *Chem. Rev.* **2004**, *104*, 4535.
(2) Petersen, M. K.; Hatt, A. J.; Voth, G. A. *J. Phys. Chem. B* **2008**, *112*, 7754.
(3) Laage, D.; Hynes, J. T. *Science* **2006**, *311*, 832.
(4) Moilanen, D. E.; Piletic, I. R.; Fayer, M. D. *J. Phys. Chem. C* **2007**, *111*, 8884.
(5) Komoroski, R. A.; Mauritz, K. A. *J. Am. Chem. Soc.* **1978**, *100*, 7487.
(6) Mauritz, K. A.; Gray, C. L. *Macromolecules* **1983**, *16*, 1279.
(7) Szentirmay, M. N.; Prieto, N. E.; Martin, C. R. *J. Phys. Chem.* **1985**, *89*, 3017.
(8) Zhao, F.; Zhang, J.; Kaneko, M. *J. Photochem. Photobiol., A* **1998**, *119*, 53.
(9) Mehata, M. S.; Joshi, H. C.; Tripathi, H. B. *Spectrochim. Acta, Part A* **2003**, *59*, 559.
(10) Lee, P. C.; Meisel, D. *J. Am. Chem. Soc.* **1980**, *102*, 5477.
(11) Szentirmay, M. N.; Martin, C. R. *Anal. Chem.* **1984**, *56*, 1898.
(12) Yeager, H. L.; Steck, A. *Anal. Chem.* **1979**, *51*, 862.
(13) Moore, R. B., III; Wilkerson, J. E.; Martin, C. R. *Anal. Chem.* **1984**, *56*, 2572.
(14) Mukherjee, T. K.; Datta, A. *J. Phys. Chem. B* **2006**, *110*, 2611.
(15) Rodríguez-Prieto, F.; Mosquera, M.; Novo, M. *J. Phys. Chem.* **1990**, *94*, 8536.
(16) Nandi, N.; Bhattacharyya, K.; Bagchi, B *Chem. Rev.* **2000**, *100*, 2013.
(17) Nandi, N.; Bagchi, B. *J. Phys. Chem. B* **1997**, *101*, 10954.
(18) Spry, D. B.; Goun, A.; Glusac, K.; Moilanen, D. E.; Fayer, M. D. *J. Am. Chem. Soc.* **2007**, *129*, 8122.
(19) Sarkar, N.; Datta, A.; Das, S.; Bhattacharyya, K. *J. Phys. Chem.* **1996**, *100*, 15483.
(20) Mukherjee, P.; Crank, J. A.; Sharma, P. S.; Wijeratne, A. B.; Adhikary, R.; Bose, S.; Armstrong, D. W.; Petrich, J. W. *J. Phys. Chem. B* **2008**, *112*, 3390.
(21) Tamoto, Y.; Segawa, H.; Shirota, H. *Langmuir* **2005**, *21*, 3757.
(22) Huppert, D.; Molotsky, T. *J. Phys. Chem. A* **2003**, *107*, 8449.
(23) Arzhantsev, S.; Ito, N.; Heitz, M.; Maroncelli, M. *Chem. Phys. Lett.* **2003**, *381*, 278.
(24) Mandal, P. K.; Paul, A.; Samanta, A. *Res. Chem. Intermed.* **2005**, *31*, 575.
(25) Druzhinin, S. I.; Bursulaya, B. D.; Uzhinov, B. M. *J. Appl. Spectrosc.* **1993**, *59*, 653.
(26) Arnett, E. M.; Quirk, R. P.; Larsen, J. W. *J. Am. Chem. Soc.* **1970**, *92*, 3977.
(27) Campillo, A. J.; Clark, J. A.; Shapiro, S. L.; Winn, K. R.; Woodbridge, P. K. *Chem. Phys. Lett.* **1979**, *67*, 218.
(28) Burai, T. N.; Panda, D.; Datta, A. *Chem. Phys. Lett.* **2008**, *455*, 42.
(29) Koti, A. S. R.; Periasamy, N. *J. Chem. Phys.* **2001**, *115*, 7094.
(30) Koti, A. S. R.; Krishna, M. M. G.; Periasamy, N. *J. Phys. Chem. A* **2001**, *105*, 1767.
(31) Chorvat, D., Jr.; Chorvatova, A. *Eur. Biophys. J.* **2006**, *36*, 73.
(32) Maroncelli, M.; Fleming, G. R. *J. Chem. Phys.* **1987**, *86*, 6221.
(33) Fee, R. S.; Maroncelli, M. *Chem. Phys.* **1994**, *183*, 235.
(34) Vajda, S.; Jimenez, R.; Rosenthal, J. S.; Fidlert, V.; Fleming, R. G. *J. Chem. Soc. Faraday Trans.* **1995**, *91*, 867.
(35) Lakowicz, J. R. *Principle of Fluorescence Spectroscopy*, 3rd ed.; Springer: New York, 2006.
(36) Lipkowitz, K. B.; Larter, R.; Cundari, T. R.; Boyd, D. B. *Reviews in Computational Chemistry*.
(37) Fletcher, A. N.; Bliss, D. E. *Appl. Phys.* **1978**, *16*, 289.
(38) Jimenez, R.; Fleming, G. R.; Kumar, P. V.; Maroncelli, M. *Nature* **1994**, *369*, 471.
(39) Vajda, S.; Jimenez, R.; Rosenthal, S. J.; Fidlert, V.; Fleming, G. R. *J. Chem. Soc., Faraday Trans.* **1995**, *91*, 867.
(40) Sen, P.; Ghosh, S.; Sahu, K.; Mondal, S. K.; Roy, D.; Bhattacharyya, K. *J. Chem. Phys.* **2006**, *124*, 204905.
(41) Mishra, P. P.; Bhatnagar, J.; Datta, A. *J. Phys. Chem. B* **2005**, *109*, 24225.
(42) Hazra, P.; Chakrabarty, D.; Sarkar, N. *Chem. Phys. Lett.* **2003**, *371*, 553.
(43) Mandal, D.; Datta, A.; Pal, S. K.; Bhattacharyya, K. *J. Phys. Chem. B* **1998**, *102*, 9070.
(44) Pal, S. K.; Peon, J.; Bagchi, B.; Zewail, A. H. *J. Phys. Chem. B* **2002**, *106*, 12376.
(45) Mandal, U.; Adhikari, A.; Dey, S.; Ghosh, S.; Mondal, S. K.; Bhattacharyya, K. *J. Phys. Chem. B* **2007**, *111*, 5896.
(46) Kivelson, D.; Friedman, H. *J. Phys. Chem.* **1989**, *93*, 7026.
(47) Lu, Z.; Polizos, G.; Macdonald, D. D.; Maniasa, E. *J. Electrochem. Soc.* **2008**, *155*, B163.
(48) Sahu, K.; Roy, D.; Mondal, S. K.; Halder, A.; Bhattacharyya, K. *J. Phys. Chem. B* **2004**, *108*, 11971.

JP907902T